

# EVALUATION OF DIAGONAL-TENSION FAILURE LOAD IN REINFORCED CONCRETE BEAMS WITHOUT STIRRUPS. CRITICAL DEPTH CRITERION

JACINTO R. CARMONA\* and GONZALO RUIZ†

\*Universidad de Castilla-La Mancha (UCLM)  
Avda. Camilo José Cela s/n, 13071 Ciudad Real, Spain  
e-mail: jacinto.rc@gmail.es, www.uclm.es

†Universidad de Castilla-La Mancha (UCLM)  
Avda. Camilo José Cela s/n, 13071 Ciudad Real, Spain  
e-mail: gonzalo.ruiz@uclm.es, www.uclm.es

**Key words:** diagonal tension failure, shear failure, reinforced concrete, size effect

**Abstract.** The present work describes a simple model, based on concepts of Fracture Mechanics, to evaluate the diagonal tension failure load in reinforced concrete beams without stirrups. It is developed by an analytical method that identifies the variables on which the diagonal traction failure depends, with special attention to bond between concrete and steel bars. The beam collapse is caused when a crack, which is developing through the beam cross section, reaches a certain depth which we will refer to as the critical depth. This depth depends on the position of the section being studied, the external load, the beam boundary conditions and the beam geometry. The presented model can help to better understand the nature of the diagonal tension failure in reinforced concrete elements without stirrups.

## 1 INTRODUCTION

The evaluation of diagonal tension failure load (shear strength) in RC elements is a problem not satisfactorily solved within the scientific and technological fields. A consensus over a mechanical model which explains simply and reasonably the behavior of the RC elements facing this type of failure and the influence of the bond between concrete and steel has not been reached so far. Nevertheless, the interest in this subject is apparent in the hundreds of publications written on it in the last fifty years and the proposed models have gradually increased their performance when compared to the experimental results. The models to determine failure load due to diagonal tension in elements without stirrups have evolved from hypotheses based on

empirical statistics [1] to truss models based on plasticity [2–6].

A new perspective to analyze the problem was introduced by Reinhardt in the eighties [7], who stated that the models and formulas to determine diagonal traction failure load should be based on Fracture Mechanics. Indeed, the brittle nature of diagonal tension failure, together with the size effect observed in tests [8, 9] and with the fact that failure is associated with crack propagation through the concrete element [10], suggest that the failure can be studied through the theories generated within the framework of fracture mechanics.

The proposed formulation assumes that diagonal tension failure is caused by the propagation of flexural cracks. Beam failure occurs

when a flexural crack reaches a certain depth, which we call *critical depth*, that depends on the crack position and on the boundary and loading conditions. This failure criterion is based on experimental observations [10], and in the results obtained with analytical models [11]. In these investigations, it has been observed that cracks initially progress in a stable manner. When one of them reaches its critical depth, it becomes to unstable, which means that the crack length increases consuming only energy stored in the specimen, with no need of additional external energy. As the model is based on Fracture Mechanics concepts, it reproduces the size-effect observed in the experiments and the influence of the variables that govern the failure, especially the bond between the reinforcing bars and the concrete matrix, the reinforcement ratio and the mechanical properties of steel and concrete.

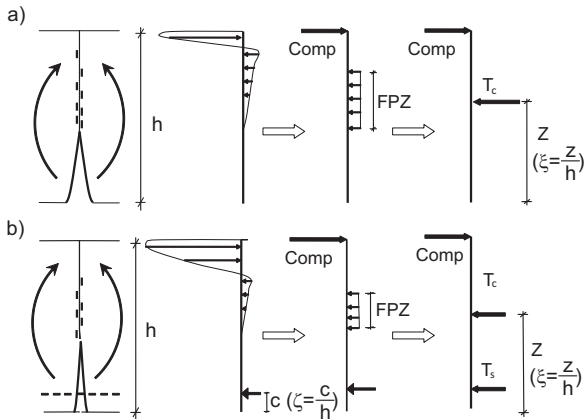


Figure 1: Bending analysis: a) plain concrete section; b) reinforced concrete section

## 2 MODELING SHEAR CRACK PROPAGATION

A three point bending beam (TPB) is considered where a vertical crack grows at a point in the shear span. The different geometric variables relevant to the problem are displayed in Figures 1 and 2. The beam has a depth  $h$ , a width  $b$  and a shear span equal to  $l$ , (which is the horizontal distance between the load point and the closest support). The depth of the crack is represented as  $z$  and the reinforcement cover as  $c$ . All these dimensions can be expressed in a

nondimensional way dividing by the depth  $h$ . In this manner we define  $\xi = \frac{z}{h}$  as the nondimensional depth and  $\zeta = \frac{c}{h}$  as the steel concrete cover expressed in nondimensional form; these parameters have a value between 0 and 1. We will also consider two additional parameters, which are the slenderness of the shear span, that is defined as  $\lambda = \frac{l}{h}$ , and another one that indicates the distance of the crack to the beam support,  $\alpha = \frac{x}{l}$ , where  $x$  is the horizontal distance from the crack to the support.

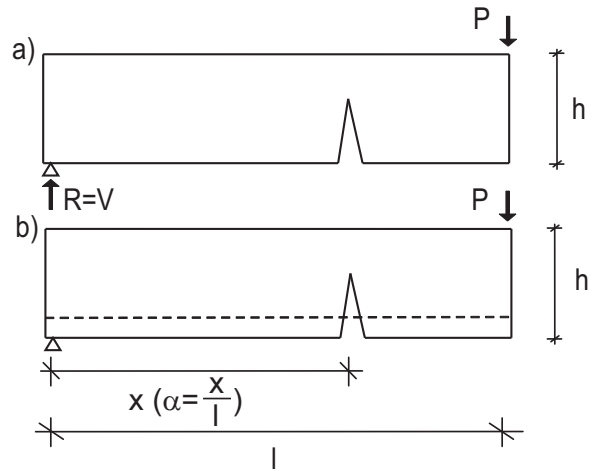


Figure 2: Beam geometry: a) plain concrete; b) reinforced concrete.

During the crack growth a damage zone is generated at the crack front. This zone is called *Fracture Process Zone (FPZ)*, shown in Fig. 1. As a simplification, in our model it is considered that tension is constant along the *FPZ*. The value of the total traction force,  $T_c$ , that is generated in the cohesive zone is equal to the area of the *FPZ* by the concrete tensile strength. The size of this zone can be expressed relative to the depth of the element through Bažant's law [12]. The traction load can be nondimensionally expressed as shown in Eq. (1). The traction force is considered to be situated at the centroid of the *FPZ*,  $z$ , see Fig. 1a. So, Eq. (1) reads as:

$$T_c^* = \frac{T_c}{bhf_{ct}} = \frac{FPZ}{h} = \frac{(1 - \xi)}{\sqrt{1 + \frac{\beta_H}{\beta_0}}}, \quad (1)$$

where  $\beta_H$  is the named Hillerborg's brittleness number [13], which is defined as the ratio between the depth of the beam,  $h$ , and the material characteristic length,  $\ell_{ch}$ , which is defined as  $\ell_{ch} = \frac{E_c G_F}{f_{ct}^2}$ , where  $E_c$  is the elasticity modulus of concrete,  $G_F$  is the fracture energy and  $f_{ct}$  is the tensile strength.  $\beta_0$  is a constant related to the aggregate size. In our case, the study was carried out taking twice the maximum aggregate size divided by  $\ell_{ch}$  [14]. In order to apply Bažant's law, we consider that the value of the tensile strength is approximately equal to the value of tensile strength for a 0-size specimen.  $\beta_H$  is used as a comparison parameter for size effect.

Equation (1) indicates that for small values of  $\beta_H$ ,  $FPZ$  occupies all the uncracked ligament and for high values of  $\beta_H$  the  $FPZ$  must be very short in relation to the beam's depth. With the aim of simplifying the model, it is considered that the compression force is located at the top of the beam. As will be explained later, this simplifying assumption does not introduce a significant error at failure.

Bending moment for a certain crack depth can be evaluated by multiplying the compression force,  $T_c$ , by the distance between the midpoint of the  $FPZ$  and the upper part of the section ( $h - z$ ) as shown in Fig. 1a.

$$M_c^* = \frac{M_c}{bh^2 f_{ct}} = T_c^* (1 - \xi) = \frac{(1 - \xi)^2}{\sqrt{1 + \frac{\beta_H}{\beta_0}}}. \quad (2)$$

The bending moment is also equal to the reaction at the support multiplied by the distance to the crack, see Fig. 2a. As the reaction in the support is equal to the shear in a TPB beam, we can state:

$$M_c = Vx = V\alpha\lambda h \implies M_c^* = V_c^* \alpha\lambda. \quad (3)$$

Substituting Eq.(3) in (2) we obtain the shear, which is expressed as:

$$V_c^* = \frac{V_c}{bh f_{ct}} = \frac{1}{\alpha\lambda} \frac{(1 - \xi)^2}{\sqrt{1 + \frac{\beta_H}{\beta_0}}}. \quad (4)$$

Concrete elements are usually reinforced by steel bars located to resist tension. The reinforcement introduces a new force,  $T_s$ , in our section, as shown in Fig. 1b. The value of this force,  $T_s$ , is equal to the steel area,  $A_s$ , multiplied by the tension in the bars,  $\sigma_s$  (Eq. (5)). The force in the reinforcement can be expressed in dimensionless form by dividing it by the section area and the concrete tensile strength:

$$T_s = A_s \sigma_s \implies T_s^* = \frac{T_s}{bh f_{ct}} = \frac{A_s \sigma_s}{bh f_{ct}} = \rho \sigma_s^*, \quad (5)$$

where  $\rho$  is the reinforcement ratio and  $\sigma_s^*$  is the tension in the reinforcement expressed in non-dimensional form. As mentioned before, to simplify the model we opt for maintaining the compression force located on the top of the cross section. In the range of steel-ratios for which the shear failure occurs, the resultant of the compression forces is close to the top and, thus, our assumption is reasonable since the error in the calculated failure load is small. Considering the above discussion, the value of the bending moment for a defined crack depth  $z$  can be written as:

$$M_t = M_c + M_s = T_c(h - z) + T_s(h - c). \quad (6)$$

Re-writing Eq. (6) in non-dimensional form:

$$M_t^* = M_c^* + M_s^* = \frac{(1 - \xi)^2}{\sqrt{1 + \frac{\beta_H}{\beta_0}}} + \rho \sigma_s^* (1 - \zeta). \quad (7)$$

Finally, using Eq. (3), the shear can be expressed as:

$$V_t^* = \frac{V_t}{bh f_{ct}} = \frac{1}{\alpha\lambda} \left[ \frac{(1 - \xi)^2}{\sqrt{1 + \frac{\beta_H}{\beta_0}}} + \rho \sigma_s^* (1 - \zeta) \right]. \quad (8)$$

It should be noted that Eq. (8) indicates that the shear is the sum of two terms. The first one depends on the concrete material properties, whereas the other one depends on the reinforcement ratio, on the tension in the steel bars

and on the concrete cover. The sum of these terms is multiplied by another term which takes into account the slenderness and the crack front position in the beam. All of the values in (8), are known but the steel tension.

To evaluate the steel tension during crack growth we need to pose an additional equation by enforcing the compatibility of displacements between concrete and steel, which implies that the crack opening is equal to the stretching of the reinforcement bars. It is assumed that the traction force of the reinforcement is equal at both faces of the crack, as shown in Fig. 3 and Eq. (9). Other compatibility equations could be considered, for example, based on the Navier hypothesis or depending on the crack opening, as done in [15]. Nevertheless, in this work we have selected Eq. (9) because it allows to include bond between concrete and steel as a variable in the problem. It is written as:

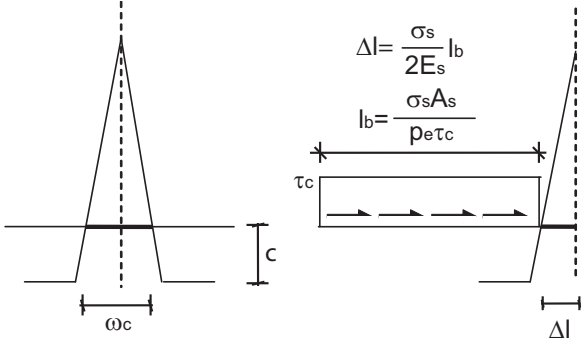


**Figure 3:** Compatibility of displacements

$$\frac{\omega_c}{2} = \Delta l, \quad (9)$$

where  $\omega_c$  is the crack opening and  $\Delta l$  is the stretching of the steel bar. We consider that steel is elastic-plastic and, so, once the tension in the reinforcement reaches the tensile strength,  $f_y$ , it remains constant during crack propagation. Equation (9) can be expressed in a non-dimensional way by dividing both terms by the depth of the beam:

$$\frac{\omega_c}{2h} = \frac{\Delta l}{h} \implies \frac{\omega_c^*}{2} = \Delta l^*. \quad (10)$$

The non-dimensional crack opening,  $\omega_c^*$ , can be evaluated by the expression given by Tada, Paris and Irwing [16]. An additional term,  $1 - \frac{\zeta}{\xi}$ , to take into account the concrete cover has been introduced:

$$\frac{\omega_c^*}{2} = \frac{\omega_c}{2h} = 12 \alpha \lambda V_t^* \frac{f_{ct}}{E_c} \xi f(\xi) \left(1 - \frac{\zeta}{\xi}\right), \quad (11)$$

where  $f(\xi)$  is equal to:

$$f(\xi) = 0.76 - 2.28 \xi + 3.87 \xi^2 - 2.04 \xi^3 + \frac{0.66}{(1 - \xi)^2}. \quad (12)$$

The stretching of the bar (Fig. 3) can be expressed by:

$$\Delta l_s^* = \frac{\Delta l_s}{h} = \frac{\sigma_s^2 A_s}{2 \tau_c E_s p_e h} = (\sigma_s^*)^2 \frac{f_{ct}^2}{2 \tau_c E_s p_e h}, \quad (13)$$

where  $\tau_c$  is the bond strength between steel and concrete, which is considered constant along the adherence length, and  $p_e$  is the bar perimeter. Substituting Eqs. (11) and (13) in Eq. (10) we obtain that the non-dimensional tension on the reinforcement can be expressed as:

$$(\sigma_s^*)^2 = 24 V_t^* \alpha \lambda \eta^2 \beta_H \xi f(\xi) \left(1 - \frac{\zeta}{\xi}\right), \quad (14)$$

where  $\eta$  is the non-dimensional bond defined by Ruiz [15], which can be written as:

$$\eta = \sqrt{n \frac{\tau_c p_e \ell_{ch}}{f_{ct} A_s}}. \quad (15)$$

Where  $n$  is the ratio between the elastic modulus of steel and that of concrete. Non-dimensional bond strength has a value that varies between 15 for smooth bars to 50 for ribbed (adherent) bars.

To evaluate the shear force and the tension in the steel bars we finally have a system of two equations, Eq. (8) and Eq.(14), which can be solved analytically. When the reinforcement

traction reaches the yield strength, the shear strength is obtained just from Eq. (8).

It should be noted that the proposed model is valid for low and medium reinforcement ratios. For high ratios the failure is caused by excessive compressions below the load bearing point, and studying this type of failure is outside of the scope of the paper. Finally, we assume that a crack may form at any point along the shear span, which is specially true for ribbed reinforcement.

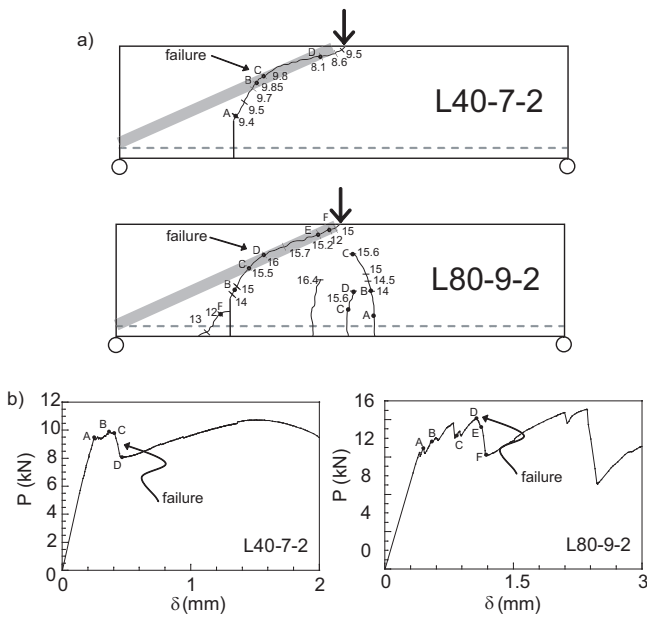


Figure 4: Failure criterion, experimental results: a) crack patterns; b)  $P - \delta$  curves

### 3 FAILURE CRITERION

Equation (8) indicated the shear force for crack propagation,  $V_t$ , but shear failure,  $V_F$ , will occur only for a definite crack depth. This depth will be referred from here as *critical depth*,  $\xi_{crit}$ . A criterion to determine  $\xi_{crit}$  can be derived from experimental observations. We base it on the experimental results carried out by Carmona, Ruiz and del Viso [10]. This experimental program was designed so that only one single mixed-mode crack generated and propagated through the specimen, as opposed to the usual dense crack pattern found in most of the tests reported in the scientific literature. In Fig. 4 we show two of the results that will help to explain the failure criterion.

Figure 4a shows the crack patterns in two of the tests. The marks and figures on the sketch refer to the corresponding points in the  $P - \delta$  curves, as shown in Figure 4b, and to the load in kN that the beam was standing when the crack tip reached that position. During the crack progress, a change in the nature of the crack propagation was observed and a subsequent unstable crack branch began leading to the beam failure. This phenomenon was associated with the so-called diagonal tension failure. This change in the nature of crack propagation can be observed in point C of beam L40 and point D of beam L80. These points shown in Figure 4a, are approximately located on the line that joins the loading point with the point where the reinforcement reaches the support. This line coincides with an ideal strut that connects the loading point to the support. These experimental observations were also assumed in an analytical model proposed by Carpinteri Ventura and Carmona [11]. Therefore, for three point bending flexure, the critical depth is defined by the line connecting the loading bearing point to the point where the reinforcement reaches the support. Mathematically it can be expressed as follows:

$$\xi_{crit} = \zeta + \alpha(1 - \zeta). \quad (16)$$

This failure criterion is associated with three point bending flexure, but can be easily generalized for any boundary and load conditions. For example for a simply supported beam subjected to a uniformly distributed load, the bending moment diagram variation is parabolic with a maximum at midspan. The critical crack variation will be also parabolic. At the maximum bending moment point the critical crack is equal to the beam depth, and in the support is equal to the cover, please see Fig. 5b.

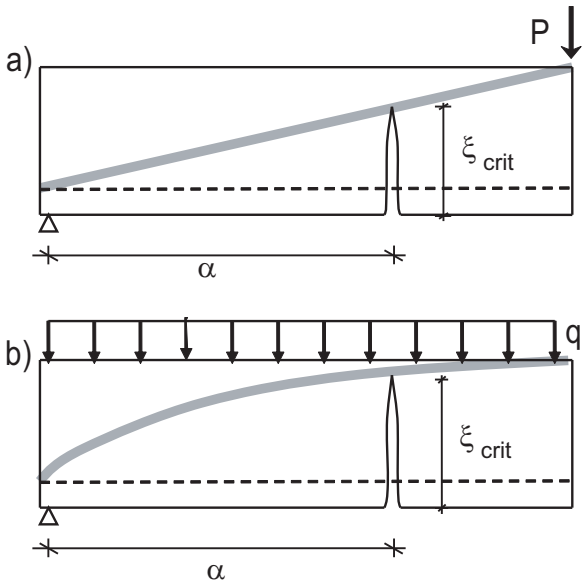


Figure 5: Failure criterion: a) three point bending; b) uniformly distributed load

Therefore, we propose that the critical depth be related to the bending moment diagram: For the maximum bending moment position the critical depth is equal to the beam depth ( $\xi_{crit} = 1$ ), and when the bending moment is equal to zero the critical depth is equal to the reinforcement concrete cover. In between, the critical depth is proportional to the value of the bending moment at that position.

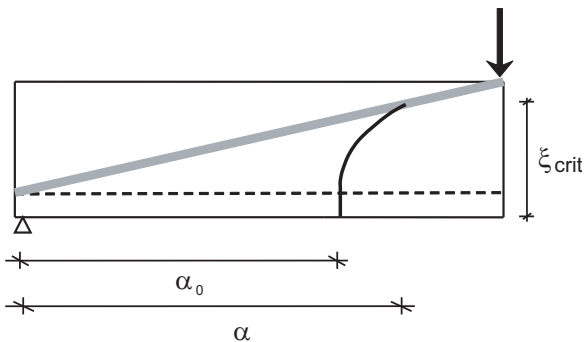


Figure 6: Crack shape

#### 4 CRACK SHAPE

So far we have considered that cracks grow in a vertical manner from the initiation point. In reality, cracks have curved trajectories approximately following the lines indicating the direction of the maximum compression. This effect

means that the initial abscissa of the crack,  $\alpha_0$ , is not the same that the abscissa of the crack tip when it reaches the critical depth,  $\alpha$ . In order to consider this mismatch, equations defining trajectory patterns can be used, as shown on Eq.(17). These equations were proposed in reference [11].

$$\alpha(\zeta, \xi) = \begin{cases} \alpha_0 & (*) \\ \alpha_0 + \left(\frac{\xi - \zeta}{1 - \zeta}\right)^\mu (1 - \alpha_0) & (**) \end{cases} \quad (17)$$

$$(*) \quad 0 \leq \xi \leq \zeta$$

$$(**) \quad \zeta \leq \xi \leq 1$$

The above formula assumes a straight trajectory from the initiation point to the reinforcement; and a parabolic trajectory which reaches the load bearing point. Through Eq. (17), a relation between the crack depth  $\xi$  and the initiation point,  $\alpha_0$ , is determined. For tree point bending, exponent  $\mu$  is equal to:

$$\mu = \frac{1}{1 - \alpha_0}. \quad (18)$$

This equation was obtained from the experimental tests performed by Carpinteri, Carmona and Ventura [17]. The failure criteria for curved cracks remain the same as for straight cracks: Once the critical depth is reached the element fails (Fig. 6).

## 5 RESULTS AND DISCUSSION

### 5.1 Model response and experimental validation

In this section it will be shown how the value of the initial crack position,  $\alpha_0$ , affects the shear strength. A beam under three point bending is modelled. Figure 7 shows the geometry and material properties. It is supposed that cracks grow in a vertical manner. The  $x$ -axis represents the non-dimensional depth,  $\xi$ , and the  $y$ -axis the non-dimensional shear strength during crack growth,  $V_t^*$ . A curve is determined for each crack initiation position. It is well known that the crack growth may present stable or unstable behavior. When the crack growth

is stable, an increase in the crack depth requires a load increase to fulfil the model equations. Conversely, unstable crack growth leads to load decrease. If we observe the curve for  $\alpha_0 = 0.2$ , after crack initiation, an unstable branch is observed. When the crack reaches the reinforcement a jump in the load is detected and, afterwards, another unstable branch takes place. There exists a minimum beyond which growth becomes stable. From this point on, shear increases until the reinforcement yields and the flexural capacity of this beam section is reached.

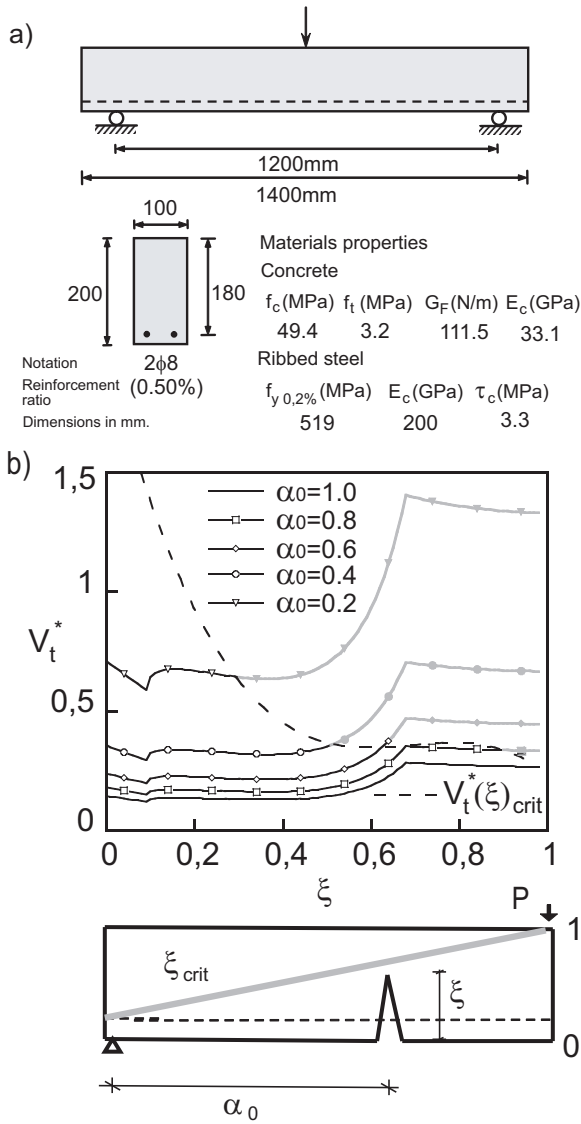


Figure 7: Model response: a) Geometry and materials properties; b)  $V_t-\xi$  curves

The behavior obtained with the model is analogous to the one described by Carpinteri as a shear version of his *Bridged Crack Model* [18]. The black part of the curve describes the shear resistance variation during the crack process until critical depth is reached, as shown in Fig. 7b. The point where the crack front reaches the critical depth indicates the shear failure or shear strength.

For cracks which form closer to the support, we observe that the failure occurs prior to reinforcement yielding (brittle failure, diagonal tension), whilst for the ones away from the support, the failure occurs after reinforcement yielding (flexural failure). It was observed that once the reinforcement has yielded, there can also be a brittle failure, just as shown by Muttoni, Rodrigues and Ruiz. [19]. In case the crack is located under the loading point, as the critical depth is equal to the depth, a brittle failure caused by diagonal tension cannot occur.

To validate the model's response, we have compared the results obtained with those of a recent experimental program performed by Carpinteri, Carmona and Ventura [17]. Sixteen geometrically similar beams, reinforced with 4 different reinforcement ratios where tested, see Fig. 8a. In this experimental program the initial position and the shape of critical cracks were studied for different reinforcement ratios. The bond strength between concrete and steel was not measured in the experimental program and, so, it has been estimated using the formulation established in the Model Code (CEB-FIB). The resulting value is 3.4 MPa. The continuous lines represent the model's response while the symbols represent the experimental results.

Figure 8b shows the comparison between theoretical and experimental results.  $X$ -axis corresponds to the initial position of the cracks, whereas  $y$ -axis represents the shear when the crack reaches the critical depth (shear strength),  $V_F^*$ . To facilitate the comparison some crack patterns of the tests are drawn at the bottom of the figure. These crack patterns are scaled 50% in the vertical axis.

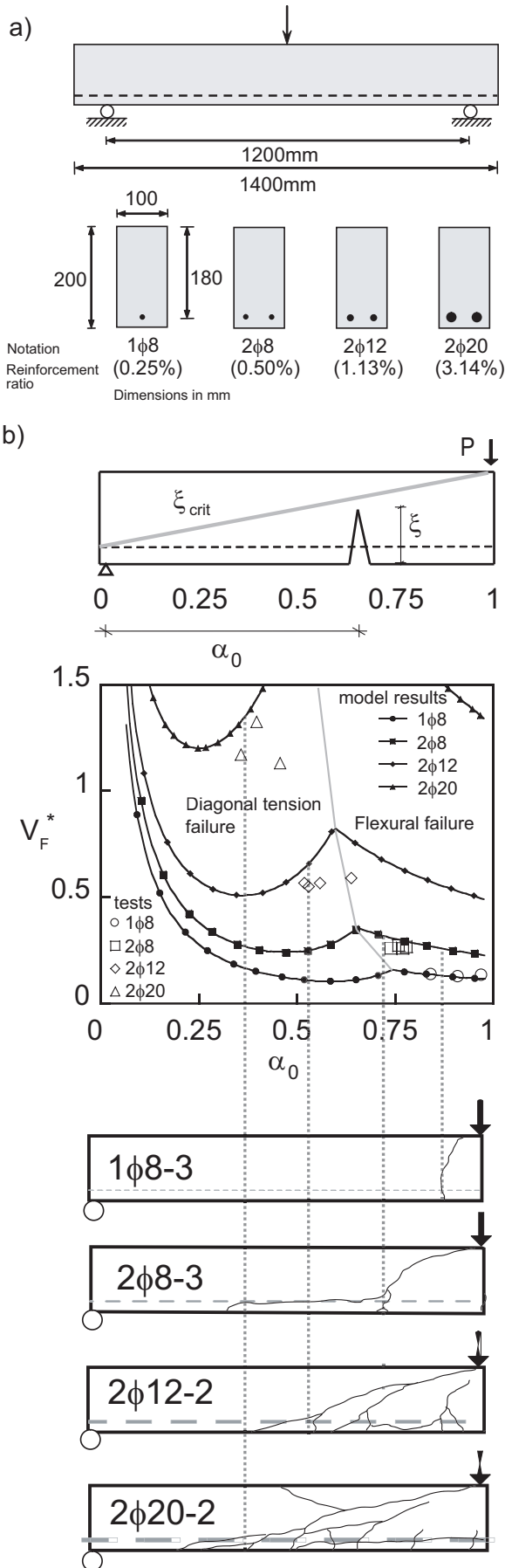


Figure 8: Model response: a) Beam geometry; b) experimental results vs. model,  $V_F - \alpha_0$  curves

To describe the model's response we are going to focus on the curve corresponding to a beam reinforced with  $2\phi 12$ , starting from the section corresponding to the load application point ( $\alpha_0 = 1$ ). For the crack under the loading point, the rebar yields before the crack reaches the critical depth and the failure is by flexure. Distancing the initiation of the crack from the bearing point, we observe that the shear strength increases, since the reinforcement gets more load and may even yield before the critical depth is attained. For a certain point,  $\alpha_Y$ , a maximum value on the curve is detected. This maximum indicates the point at which the rebar reaches its yield strength exactly at the same time that the crack reaches the critical depth. For values of  $\alpha_0$  lower than  $\alpha_Y$  the rebar has not yielded when the crack tip reaches the critical depth and the beam failure occurs by diagonal tension. The shear strength decreases until reaching a minimum for a certain initiation point, situated in our case for  $\alpha_0 = 0.4$ . This minimum has also been found in experimental results, as Kim and White reported in references [20, 21]. For cracks with an initiation point closer to the support, the shear strength starts to increase although the critical depth is low. It should be noted that the actual shear strength of the beam has to be the smallest shear found varying  $\alpha_0$ .

The shape of the curve obtained with the model, showing a minimum in the central part of the shear span, fits the description proposed by Kani and Wittkopp [22]. In the zone near to the support we find an area where the failure is produced by yielding of the rebars (flexure); but if we move away from the support along the shear span the failure occurs during the development of a crack (diagonal tension). In some conditions there also can be a failure due to diagonal compression close to the support, this type of failure is not considered in the model though.

Figure 8 shows that for low reinforcement ratios (e.g.  $1\phi 8$ ) the failure take place in sections near the loading point, where the steel reaches

the elastic limit before the crack grows to the critical depth. Upon increasing the reinforcement ratio, the critical section moves away from the load application point to positions where the steel does not yield. The experimental tendency is captured by the model and even the shear loads obtained match quite reasonably the experimental ones. More over, the model explains the “valley” in the shear resistance along the beam longitudinal axis. In the results obtained for the largest reinforcement ratio ( $2\phi20$ ) the differences between the model and the experiments are conditioned by the type of failure, since in highly reinforced beams the failure is produced by excessive compression and not by diagonal tension.

## 5.2 Size effect

Figure 9 shows the model’s response when varying the element size. We compare the response for two different values for the crack initiation: One which starts at the middle of the shear span,  $\alpha_0 = 0.5$  (diagonal tension failure), and the other for the crack produced under the load point,  $\alpha_0 = 1.0$  (flexural failure). The mechanical properties for this example are the same as those used in beam with  $2\phi12$  reinforcement from the previous section. The  $x$ -axis represents the element size in terms of the Hillerborg’s brittleness number. The usual range of this parameter in structures is indicated with two vertical lines. The  $y$ -axis represents the shear strength.

For the crack located at  $\alpha_0 = 0.5$  there exists a strong size effect, i. e. the shear strength depends on the element size, which is caused by the existence of a fracture process zone in the crack front. For the asymptotic behavior, the curve presents a 0-slope curve, that is size effect disappears as much with smaller sizes than with bigger ones. For the crack located at  $\alpha_0 = 1.0$ , shear strength does not present any size effect, since the reinforcement yields before the crack reaches the critical depth and the tractions in the *FPZ* do not contribute much to the ultimate load. The results obtained with the model coincide with the experimental observations in those

cases where the flexural failure involving reinforcement yielding does show an effect of scale, whereas in the diagonal tension failure this size effect is indeed noticeable.

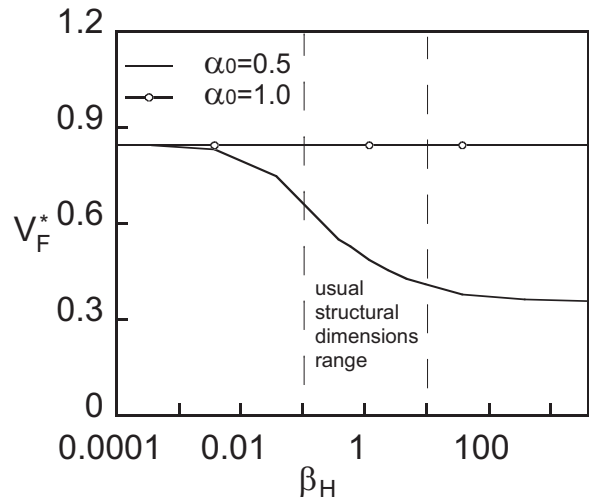


Figure 9: Size effect

## 5.3 Bond effect

Figure 10 shows the model response for variations in the bond between concrete and steel. It represents the crack depth versus the shear that produces crack propagation. We modeled the beam reinforced with  $2\phi12$  shown in section 5.1. When bond is increased, the crack depth for which the steel yields decreases. For low bond strength conditions (smooth bars) cracks have to develop fully before the steel yields. In the case of high adherence (ribbed bars), steel yielding occurs shortly after the crack crosses the rebar.

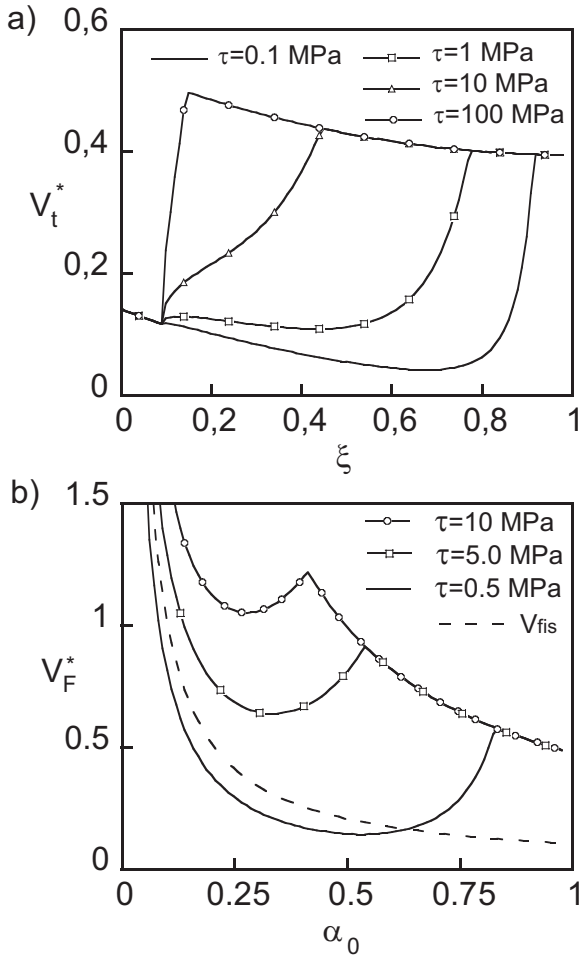


Figure 10: Bond influence: a)  $V_t-\xi$  curves; b)  $V_F-\alpha_0$  curves

In Fig. 10b,  $x$ -axis displays the initial crack position and  $y$ -axis the shear strength. When the bond strength increases, the value of  $\alpha_Y$  decreases and the shear strength increases. In the extreme case of the bond strength having an infinite value, the element fails by flexure because, for all possible cracks, the steel yields just after crossing the rebar position and, therefore, before reaching the critical depth. Fig. 10b also shows that the minimum of the curve moves towards the support as the bond strength increases. Low values for the bond strength lead to low values for the failure loads, even lower than the load that is required for fracture initiation in that particular point,  $V_{fis}$ . This means that the diagonal tension failure would be very unlikely for beams in which the steel to concrete interface is weak. Indeed,

in this case there would be cracks only under the load bearing point and there would not be crack generation nor propagation along the shear span. So, in such conditions the shear failure would not occur.

## 6 CONCLUSIONS

In this work we presented a model based on fracture mechanics concepts for studying shear strength in reinforced concrete beams without stirrups. The model shows the relation which exists between crack propagation and failure. For the model, we proposed a failure criterion based on the crack growth. When the crack reaches a definite depth, which we refer to as critical depth, the beam failure takes place. This critical depth depends on the type of loading, the boundary conditions and the beam geometry.

The proposed model identifies the variables that govern the failure, including the bond between concrete and steel. We also showed that the load for which the crack reaches the critical depth depends on the point where it initiates, besides the concrete and steel mechanical properties and the geometry of the beam section. The model explains the shear resistance variation in the cross section along the shear span, showing a minimum around the mid shear span. This fact connects with experimental observations made, among others, by Kani and Wittkopp [22].

The model reproduces the size effect that has been experimentally observed. It also explains the differences between the size effect in flexural and shear failures and describes their respective asymptotic behavior.

The theoretical development presented here can be used to study concrete elements for other load and boundary conditions. It can help to a better understanding of the nature of shear strength in reinforced concrete elements without stirrups. Finally expressions derived from this study could be used to improve shear analysis of RC beams in design Codes.

## Acknowledgements

Financial support from the *Subdirección General de Proyectos de Investigación*, Spain, through Grant MAT2009-12023 is greatly appreciated.

## REFERENCES

- [1] T. Zsutty, Beam shear strength prediction by analysis of existing data. *ACI Structural Journal*, 65(11):943–951, 1968.
- [2] J. Schlaich, K. Schafer and M. Jennewein, Toward a consistent desing of structural concrete. *Journal Prestressed Concrete Institute*, 32(3):74–150, 1987.
- [3] T. Hsu, *Unified Theory of Reinforced Concrete* CRC Press, Boca Raton. 1993.
- [4] M. P. Collins and D. Kuchma, How safe are our large, lightly reinforced concrete beams slabs and footings?. *ACI Structural Journal*, 99(4):482–490, 1999.
- [5] F. Vecchio and M. Collins, Predicting the response of reinforced concrete beams subjected to shear using the modified compression field theory. *ACI Structural Journal*, 105(2):163–172, 2008.
- [6] A. Muttoni and M. F. Ruiz, Shear strength of members without transverse reinforcement as a function of the critical shear crack width. *ACI Structural Journal*, 85(3):258–268, 1998.
- [7] H. W. Reinhardt, Similitude of brittle fracture of structural concrete, in: *Advanced Mechanics of Reinforced Concrete, IASBE Colloquium*, Delft, 175–184, 1981.
- [8] G. N. J. Kani, How safe are our large concrete beams?. *ACI proceedings Journal*, 64(3):128–141, 1967.
- [9] Z. P. Bažant and M. P. Kazemi, Size effect in diagonal shear failure. *ACI Structural Journal*, 88(3):268–276, 1991.
- [10] J. R. Carmona, G. Ruiz and J. R. del Viso, Mixed-mode crack propagation through reinforced concrete. *Engineering Fracture Mechanics*, 74(17):2788–2809, 2007.
- [11] A. Carpinteri, J.R. Carmona and G. Ventura, Propagation of flexural and shear cracks through reinforced concrete beams by the bridged crack model. *Magazine of Concrete Research*, 59(10):743–756, 2007.
- [12] Z. P. Bažant, Size effect in blunt fracture: Concrete, rock, metal. *Journal of Engineering Mechanics*, 110(4):518–538, 1984.
- [13] Z. P. Bažant, and J. Planas, *Fracture Size Effect in Concrete and Other Quasibrittle Materials*. CRC Press, Boca Raton. 1998.
- [14] Z. P. Bažant and P. Pfeiffer, Determination of fracture energy from size effect and brittleness number. *ACI Materials Journal*, 84(6):463–480, 1987.
- [15] G. Ruiz, Propagation of a cohesive crack crossing a reinforcement layer. *International Journal of Fracture*, 111(3):265–282, 2001.
- [16] H. Tada, P. Paris and G. Irwin, *The Stress Analysis of Cracks Handbook*. Del Research Corporation, 1973.
- [17] A. Carpinteri, J.R. Carmona, and G. Ventura, Failure mode transitions in RC beams. Part 2 experimental tests. *ACI Structural Journal*, 108(3):286-293, 2011.
- [18] A. Carpinteri, Stability of fracturing process in RC beams. *Journal of Structural Engineering-ASCE*, 110:544–558, 1984.
- [19] A. Muttoni, R.V. Rodrigues and M.F. Ruiz, Influence of shear on rotation capacity of reinforced concrete members without shear reinforcement. *ACI Structural Journal*, 107(5):516–525, 2010.

- [20] W. Kim and R.N. White, Shear-critical cracking in slender reinforced concrete beams. *ACI Structural Journal*, 96(5):757–5765, 1999.
- [21] W. Kim and R.N. White, Hypothesis for localized horizontal shearing failure mechanism of slender RC beams. *Journal of Structural Engineering - ASCE*, 125(10):1126–1135, 1999.
- [22] M.H.M. Kani and R. Wittkopp *Kani on Shear in Reinforced Concrete*. Department of Civil Engineering, University of Toronto, ON, Canada, 1979.